Osmotic squat actuation in stiffness adjustable bacterial cellulose composite hydrogel

ARTICLE

Osmotic squat actuation in stiffness adjustable bacterial cellulose composite hydrogel

Chen Qian, Taka-Aki Asoh*, Hiroshi Uyama*

Mechanically adaptive hydrogels can change their mechanical characteristics in response to external stimuli and show potential applications in biomechanical fields. To eliminate the undesired swelling/shrinkage in the responding process, poly(acrylic acid) (PAA) was grafted to acryloyl chloride (AC)-modified bacterial cellulose (BC) by free-radical polymerization. The obtained BC-*g*-PAA composite hydrogels showed adjustable stiffness in compression, kept soft at pH lower than 6 (compression strain over 49% at a stress of 0.1 MPa), and stiffened when pH reached 7 (compression strain lower than 27% at a stress of 0.1 MPa), while the volume change ratio was consistently lower than 15%. Based on this, the hydrogel showed interesting squat actuation to lift a weight. The BC composite hydrogel exhibited dual pH-responsiveness after grafting PAA with poly[2-(dimethylamino)ethyl methacrylate], confirmed the general availability of this strategy in fabricating volumetrically stable and mechanically adaptive hydrogels. The surrounding solution-independent softening of BC-*g*-PAA hydrogel was observed in 8 min under UV irradiation via a photo-triggered pH jump reaction. By virtue of the selective UV irritation, the spatiotemporally controllable softening with actuation in BC-*g*-PAA hydrogel was realized. The developed pH-responsive mechanically adaptive BC composite hydrogels with high dimensional stability and UV-activated spatiotemporal squat actuating capability are expected to provide more options in developing novel bioimplants and smart structures.

1. Introduction

Smart materials are well-designed materials that can adjust their characteristics in response to external stimuli, show extensive applications in actuators, sensors, biomedical devices, and other smart structures[1-4]. Among them, smart hydrogels, which have the advantages of high water content, soft tissue-mimicking consistency and high permeability to metabolites and oxygen, showed widespread applications in biomedical devices and soft actuators[5-9].

Recently, attempting to design novel smart hydrogels with tunable mechanical properties has generated considerable research interest. In response to external stimuli, the smart hydrogels were expected can dynamically adjust their mechanical characteristics to match human soft tissues or regulate cell proliferation and differentiation, which could facilitate the application of hydrogels in biomedical devices, drug delivery, cell proliferation, and tissue engineering[10-12].

Continuous attempts have been made by scientists to develop novel mechanically adaptive hydrogels through different strategies, such as utilizing hydrogen bonding[13], ionic cross-linking[14], conformational changes in proteins[15] and other dynamic bonds to regulate the topology of a hydrogel network[16]. Up to now, the mechanical adaptivity of hydrogels still relies mainly on the variation of crosslinking density in hydrogel network or tuning conformation of polymer chains between the crosslinking points, which will give rise to a concomitant 1swelling/shrinkage with mechanical property change. The concurrent drastic swelling and shrinkage would restrict their applications in biomechanical fields, because the undesired volume change hinders the precise control of the shape in hydrogel implant, moreover, causes displacement from the installation site, irritation and even damage to the surrounding tissues[17-19]. Thus, successes in developing mechanically adaptive hydrogels with high dimensional stability could promote the design of the next generation of body implant materials[11].

Department of Applied Chemistry, Graduate School of Engineering, Osaka University, 2-1 Yamadaoka, Suita, Osaka 565-0871, Japan.
E-mail: asoh@chem.eng.osaka-u.ac.jp, uyama@chem.eng.osaka-u.ac.jp

ARTICLE
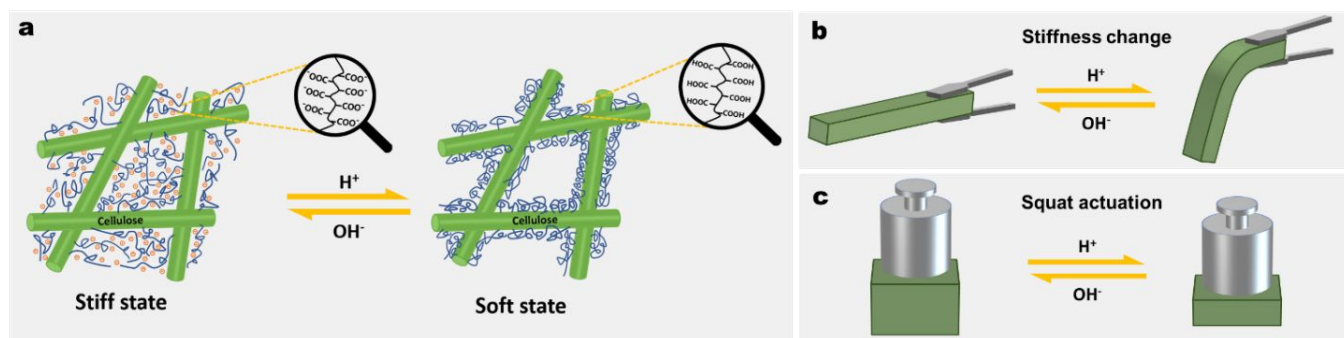
Fig. 1 (a) Mechanism of pH-induced stiffness change behavior in BC-*g*-PAA hydrogels: protonation and ionization of PAA with internal osmotic pressure change. Illustration of the reversible pH-responsive (b) stiffness change and (c) squat actuation in BC-*g*-PAA composite hydrogels.

On the other hand, smart hydrogels with stimuli-responsive swelling/shrinkage have been developed as soft actuators, which attracted increasing attention due to their promising potential applications in biomedicine, and soft robotics, and as artificial muscles[20, 21]. The main principle of actuation performance in hydrogel actuators is based on the asymmetric swelling of their various inhomogeneous structures[22, 23]. Based on the most well-known reversible bending and folding in laminated layer hydrogel actuators[24-28], more sophisticated shape deformations of the advanced hydrogel actuators can be programmed by assembling hydrogel building blocks[29, 30] and photolithographic patterning[31, 32]. However, subject to the nonuniform swelling mechanism, shape deformations in common hydrogel actuators happen in at least two directions, makes them unable to operate even simple unidirectional actuation instead. Unidirectional actuation of hydrogels, such as squat or vertical lifting, would provide more options in soft robotics and smart structure design.

An ionic strength-responsive stiffness adjustable bacterial cellulose (BC)/poly(sodium styrene sulfonate) (PSS) composite hydrogel based on a new mechanism was reported in our previous study[33]. It utilized BC as a matrix and grafted PSS as an osmotic pressure generator, showed significant stiffness change without any obvious volumetric changes in prepared BC-*g*-PSS composite hydrogel. BC is a biocompatible hydrogel consisting of highly developed cellulose nanofibrillar structures, which is usually obtained by microbial fermentation in static[34, 35]. The stable cellulose nanofibrillar network in BC could eliminate the potential swelling/shrinkage, while the grafted ionic strength-responsive PSS causing a variation in interior osmotic pressure to adjust the stiffness of the BC-*g*-PSS composite hydrogel.

The strategy for preparing dimensionally stable stiffness adjustable BC composite hydrogel was retained in this study. New types of pH-responsive mechanically adaptive BC composite hydrogels were prepared, not only conventional single-pH responsiveness but also dual-pH responsiveness and remote UV-triggering were showed. Systems that can response to pH environment are of particular interest for biomedical applications as several locations in the body exhibit substantial pH changes during either normal function or as part of a disease state[36]. Furthermore, remote triggering would provide convenience and practicability. Poly(acrylic acid) (PAA) was grafted onto BC for responding to the pH change of surrounding

solutions *via* dramatical protonation and ionization (illustrated in **Fig. 1a**). The stiffness of BC-*g*-PAA hydrogel can be adjusted by generating and eliminating internal osmotic pressure upon pH change without any obvious volumetric changes (illustrated in **Fig. 1b**). Most interestingly, BC-*g*-PAA hydrogel also showed a novel squat actuating capability with lifting a weight up and down reversibly (illustrated in **Fig. 1c**). Based on the BC-*g*-PAA hydrogels, poly[2-(dimethylamino)ethyl methacrylate] (PDMAEMA) was introduced and formed polyampholyte with PAA, extended the monotonous pH-responsibility in BC-*g*-PAA to a dually pH-responsive behavior in BC-*g*-Polyampholyte (BC-PAmph) hydrogels. Moreover, the BC-*g*-PAA hydrogel showed surrounding solution-independent self-softening and spatiotemporal actuation upon UV stimulus by utilizing a photo triggered pH-jump reaction, which may facilitate their mechanical applications for smart structural materials.

Combining with the biocompatibility of BC, the presented pH-responsive BC composite hydrogels are expected to provide new options in therapeutic implants due to a large variety of physiological pH that exists not only in normal conditions such as the gastrointestinal tract but also in pathological conditions such as tumoral culture. Moreover, the exploration in remote UV-triggering and squat actuating could further extend the application of the BC composite hydrogels as a smart structural material. This fabrication strategy of mechanically adaptive hydrogel combining dimensionally stable hydrogel matrix with free-chain stimuli-responsive polymers exhibits generalizability and may open the door to an exploration of these materials as novel biomedical implants, smart structures, and soft robotics.

2. Experimental section

2.1 Materials

Bacterial cellulose (BC) pellicles were obtained from Fujicco Co., Ltd. *N,N*-dimethyl formamide (DMF), triethylamine (TEA) and acrylic acid (AA) monomer were purchased from Nacalai Tesque. Acryloyl chloride (AC), sodium hydroxide, hydrochloric acid, and sodium chloride standard solutions were all purchased from Wako Chemicals. 2-Nitrobenzaldehyde and 2-(dimethylamino)ethyl methacrylate (DMAEMA) monomer were obtained from Tokyo Chemical Industry. Ammonium persulfate (APS) was purchased from Sigma-Aldrich. Besides, deionized (DI) water was used for all experiments.

2.2 Purification and quantification of BC

BC hydrogels were firstly thoroughly washed by DI water, then purified in 0.2 mol L^{-1} NaOH aqueous solution at 80 °C for 4 h, finally washed with DI water until the pH value was constantly neutral. In this work, all the pristine BC gels used were counted as a composition of 1 wt% cellulose and 99 wt% water. The concentrations of solutions were the final values after adding BC gels when BC was involved.

2.3 Modification of BC with AC

Prior to modification, the BC hydrogels were subjected to a solvent exchange, replacing interior water in BC by DMF. Specifically, BC was firstly immersed in abundant DMF for 12 h. Water in the BC/DMF mixture was eliminated by rotary evaporating at 50 °C with a pressure of 30 mbar. Until no water could be collected, the solvent exchange was considered as completed. After that, distilled TEA was added into the mixture of BC and DMF, excess AC (a mole ratio of 10:1 to the hydroxy groups in cellulose) was added dropwise in the mixture while stirring in an ice bath. The reaction was conducted at room temperature for 24 h until adding deionized water to terminate the reaction. The resultant AC modified BC (ACBC) gels were purified by washing with deionized water completely.

2.4 Preparation of BC-*g*-PAA and BC-*g*-PAmph hydrogels

The PAA was grafted from ACBC *via* free-radical polymerization by using APS as initiator. The required amount of AA (was partly neutralized by NaOH) with 1.0 mol% APS (corresponding to AA monomer) was added to the mixture of ACBC and deionized water. The mixture was well homogenized by stirring for about 8 h in an ice bath before purging with gaseous N_2. Then the free-radical polymerization was initiated by transferring the mixture into a 65 °C oil bath. The polymerization was continued for 24 h. After that, the obtained BC-*g*-PAA composite gels (BC-*g*-PAA) were completely washed with deionized water before characterizations. The BC-*g*-PAA samples were denoted as BC-PAA-*x*-*y*, where *x* represents the concentration of AA in graft polymerization, *y* presents the neutralization degree of AA monomer before polymerization. BC-0 is designated as pristine BC gel. Moreover, BC-*g*-polyampholyte (BC-PAmph) hydrogels were prepared through graft copolymerization of equal AA and DMAEMA monomer in the presence of ACBC and APS, the details were consistent with the preparation of BC-PAA but without the neutralization of AA by NaOH. The BC-PAmph samples were designated as BC-PAmph-*z*, where *z* represents the overall molar concentration of monomers in graft polymerization.

2.5 Determination of the composition of BC-0 and BC composite hydrogels

The composition of BC gels was determined by weighting as follows. For BC composite gels, the initial weight of the used pristine BC gels was first recorded before modification. After grafting of stimuli-responsive polymers, the weight of

corresponding composite gels was measured again. Then, the BC composite gels were dried in an oven at 80 °C up to a constant mass, and the dried weights were measured. For BC-0 gels, the wet and dry weight were also measured.

The mass percent of water (R_w), cellulose nanofibers (R_c) and grafted polymer (R_p) in BC gels could be calculated with the recorded weight of hydrogels at hydrate and dried state, according to Eqs. (1), (2) and (3), respectively[33].

$$R_w = \frac{W_0 - W_d}{W_0} \times 100\% \tag{1}$$

$$R_c = \frac{W_c}{W_0} \times 100\% \tag{2}$$

$$R_p = \frac{W_d - W_c}{W_0} \times 100\% \tag{3}$$

In the equations, W_d is the dry weight and W_0 is the wet weight of gels. W_c is the weight of cellulose nanofibers in gels. For BC-0 gels, no grafted polymer is involved, W_c is exactly the W_d. However, it is unable to determine W_c in BC composite gels by measuring the weight directly. Therefore, the W_c in BC composite gels was estimated on the basis of initial wet weight (pristine BC gels before any modifications) with the R_c of BC-0 gels.

2.6 Characterization of BC hydrogels

Attenuated total reflection Fourier transform infrared (ATR-FTIR) spectroscopy (Thermo Scientific Nicolet iS 5, USA) was used to confirm the successful preparation of BC-*g*-PAA and BC-*g*-PAmph composite hydrogels. The samples for FTIR were frozen by liquid nitrogen and then dried in a vacuum freeze-drier for ATR-FTIR measurement.

The vertical sections of the BC and BC composite hydrogels were observed using scanning electron microscopy (SEM) (Hitachi SU3500, Japan). The hydrogel samples were freeze-dried and sputtered with gold by using an MSP-1S magnetron sputter (Vacuum Device Inc, Japan). The samples were observed under a high vacuum at an acceleration voltage of 1.50 kV.

2.7 Compression test

For the compression test, the samples were cut into cylinders (10 mm in diameter and 10 mm in height). The compressing testing of BC gels was performed by applying the respective compressive stress along the growth direction (weaker direction) of BC. The required strain to achieve a deformation speed of 3.0 mm·min^{-1} was measured in a 500 N load cell with a material tester (Shimadzu EZ Graph, Japan) at room temperature.

2.8 pH-responsive behavior of BC composite hydrogels

The original volumes of BC composite gels in DI water were firstly measured *via* volume displacement method using a measuring cylinder. Subsequently, BC composite gels were separately immersed in different pH aqueous solutions but with the same ionic strength of 0.01 mol L^{-1}, which can be readily

obtained by compounding 0.01 mol L^{-1} NaCl solutions with 0.01 mol L^{-1} HCl or 0.01 mol L^{-1} NaOH solutions. After 24 h, took out the BC gels, gently removed the excess of solution and measured their equilibrium volumes. Afterward, the compression properties of samples were measured according

Table 1 The composition of BC-g-PAA hydrogels and pH of their corresponding monomer solutions.

Sample	pH of monomer solution	Water content (wt%)	Cellulose content (wt%)	Grafted polymer content (wt%)
BC-0	-	99.4	0.6	0
BC-PAA-1.0-0	2.1	58.5	0.5	41.0
BC-PAA-1.0-60	4.5	99.0	0.6	0.4
BC-PAA-1.0-95	5.5	99.3	0.6	0.1

to the preceding method. The volume change ratio (VCR) of BC gels in ionic responding was calculated as followed:

$$VCR = \frac{V_e - V_0}{V_0} \times 100\% \qquad (4)$$

Where the V_e is the equilibrium volume of BC composite gels after being immersed in corresponding solutions and V_0 is the original volume of the as-prepared BC composite gels in DI water.

3. Results and discussion

3.1 BC-g-PAA composite hydrogels prepared with different monomer neutralization degrees

The preparation process of BC-PAA hydrogels is illustrated in **Fig. 2a**. Firstly, the acrylate groups were introduced into BC by reacting the surface hydroxyl groups of BC with acrylate chloride in the presence of TEA[33]. The graft polymerization of acrylic acid onto BC was conducted in water by using APS as initiator at 65 °C.

Before polymerization, the acrylic acid monomer was pre-neutralized to different percent neutralization by sodium hydroxide aqueous solution. The composition of BC-g-PAA hydrogels prepared with the same AA concentration of 1.0 mol L^{-1} and different pre-neutralization degrees was recorded in **Table 1**. The amount of grafted PAA in the BC-PAA composite hydrogels showed a strong dependence on the percent neutralization under the same monomer concentration, decreased with increasing percent neutralization from 0 up to

95%. The pH values of the monomer solutions before polymerization were recorded. 1.0 mol L^{-1} AA solution without neutralization showed a pH of 2.1 at room temperature, which was much lower than the pK_a of AA, as known as about 4.3. In this case, AA monomers kept the initial protonated state and associated with the BC surface prior to polymerization by the H-bonded interactions between AA monomers and surface hydroxyl groups of BC. During the polymerization, the H-bonding between AA monomers could promote the polymerization rate, resulting in a formation of PAA network inside BC hydrogels[37, 38]. Thus, the highest PAA content of 41.0 wt% was found in BC-PAA-2.0-0 gels.

With the neutralization degree increase, the PAA content of BC composite hydrogel dramatically decreased. The most likely explanation was that the ionic repulsion between the monomer and growing polymer increased, due to the increasing of ionized monomer[37-39]. Especially for BC-PAA-1.0-95, since the monomer solution showed a much higher pH, most of the monomers were ionized in aqueous solution. Therefore, BC-PAA-1.0-60 and BC-PAA-1.0-95 showed a fairly low PAA content of 0.4 and 0.1 wt%, respectively.

Moreover, it was found that the BC-g-PAA hydrogels (without washing by water) with different monomer percent neutralization showed an obvious difference in their spectra (**Fig. 2b**). In the spectrum curve of BC-PAA-1.0-0, the peak of C=O stretching located at 1720 cm^{-1} indicated the grafting of non-neutralized poly(acrylic acid) [33, 40]. With the percent neutralization increasing up to 60% and 95%, the peak of C=O stretching in carboxyl groups gradually became weaker, and a
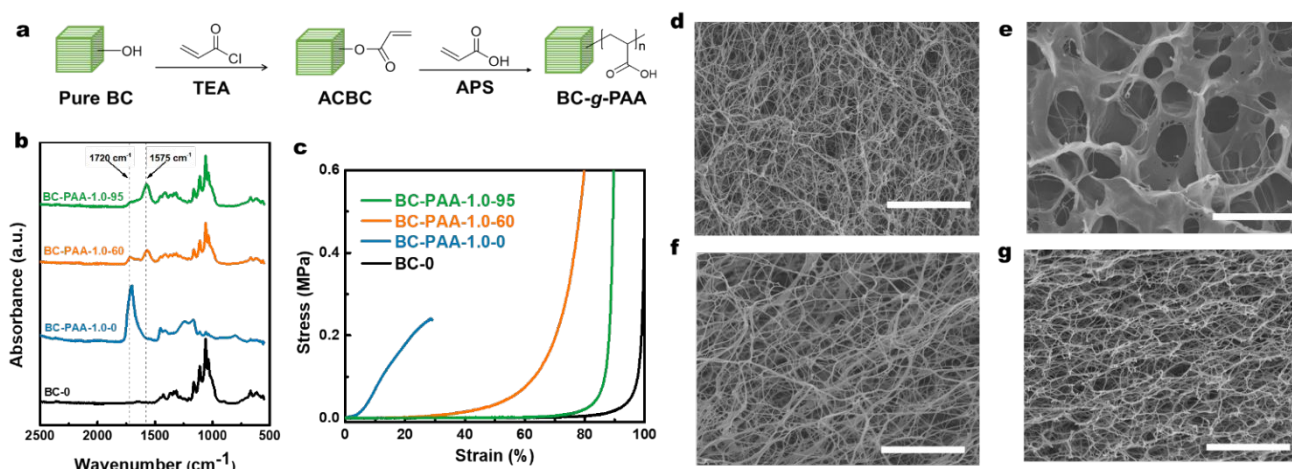
Fig. 2 (a) Schematic presentation of the preparation of BC-g-PAA. (b) ATR-FTIR spectra of BC-0, ACBC, and BC-g-PAA hydrogells. (c) Compression stress-strain curves of pristine BC and BC-g-PAA hydrogels at pH 7. SEM images of freeze-dried (d) BC-0, (e) BC-1.0-0, (f) BC-1.0-60, (g) BC-1.0-95 at 3000× magnification (scale bar: 10 μm)

new peak of -COO$^-$ asymmetric stretching vibration at 1575 cm^{-1} arose and enhanced, confirmed the different contents of ionized carboxylate groups in BC-*g*-PAA hydrogels.

With the different contents of PAA, BC-PAA composite hydrogels showed different mechanical properties at pH 7 in their compression stress-strain curves (**Fig. 2c**). Pure BC is well-known as an ultra-soft hydrogel in compression, owing to the interior porous cellulose nanofiber network (**Fig. 2d**), which is too weak to resist the external compression force. As a result, BC-0 exhibited two-region in its compression curve, which mainly includes the first plateau with stress nearly 0, and the last densification region with sharply increasing stress.

However, BC-PAA-1.0-0 showed obviously different mechanical characteristics in compression owing to the presence of PAA. As observed in **Fig. 2e**, individual cellulose nanofibers could rarely be observed; the massive PAA filled in the nanocellulose network of BC and tremendously strengthened the composite hydrogels. As a result, relatively high stress was shown in the low strain region rather than a low-stress plateau in **Fig. 2c**. Furthermore, with the filling of PAA in the internal porosities of the nanocellulose network, the morphology of solid phase in BC-PAA-1.0-0 was harder to self-adjust in compression, thus the sample was easily crushed at a low strain of 24.8%. In comparison with BC-0, an approximate linear elastic deformation region can be recognized between the first plateau and later densification region in the compression curve of BC-PAA-1.0-60, due to the strengthening effect of PAA in the composite hydrogel. Comparing to BC-PAA-1.0-0, the lyophilized BC-PAA-1.0-60 remained a porous cellulose nanofiber network with locally aggregated PAA as observed in **Fig. 2f**. BC-PAA-1.0-95, with the lowest PAA content, exhibited almost the same micromorphology (**Fig. 2g**) and a similar two-region compression curve with BC-0 but showed an earlier appeared densification region.

The strengthening effect of PAA in BC-*g*-PAA composite hydrogels can be divided into two parts. Firstly, the carboxylic groups of grafted PAA would get deprotonated at a pH > pK_a, and Na$^+$ counterions (introduced during the pre-neutralization process of monomer) would disperse to the abundance of water, negatively charged carboxylate ions would be generated in BC-PAA composite, as illustrated in **Fig 1a**. In this case, the BC-PAA hydrogels would be highly strengthened because of the large osmotic pressure generated inside by the presence of the carboxylate ions, arising a stress increase in the low strain region. Secondly, the grafted PAA polymer would enhance the nanocellulose network of BC matrix through the physical entanglement of BC and PAA chain along with the formation of hydrogen bonds or directly filling in the voids and gaps of the nanocellulose network. Thus, the densification region would appear earlier in compression curves.

3.2 pH-responsiveness of BC-*g*-PAA composite hydrogel

The pH-responsive mechanical adaptivity of the BC-*g*-PAA composite hydrogels was preliminarily studied at pH 2, 7 and 12. The underlying mechanism was illustrated in **Fig. 1a**. When the pH of the surrounding solution decreased from 7 to 2, the ionized carboxylic acid groups of grafted PAA would be protonated. The amount of negatively charged groups in BC-PAA gels would dramatically decrease due to the transformation from carboxylate groups to carboxy groups. Therefore, the generated osmotic pressure in BC-PAA would disappear, and further turn BC-PAA to its soft state.

However, BC-PAA-1.0-0 showed an unanticipated stiffness change behavior along with pH (**Fig. 3a**). It is noticeable that the content of PAA in BC-PAA-1.0-0 was 41.0 wt%, because of the strong H-bonding effect between unneutralized AA monomers and BC. The PAA-dominated structure of BC-PAA-1.0-0 was well observed in **Fig. 2e**. As aforementioned, it could be considered that PAA well filled the nanocellulose network in BC as a secondary hydrogel, rather than simply grafting on the surface. BC-PAA-1.0-0 showed a stiff state at pH 7 because of the high solid content in the composite hydrogel, which played a dominant role in BC-PAA-1.0-0. After pH increased to 12, PAA started to swell because of the electrostatic repulsion generating from the negatively charged carboxylate groups, broke the barrier of BC, made BC-PAA-1.0-0 swollen to 273.7% of its original volume and turned the composite gel to brittle, just like the common pH-responsive poly(acrylic acid) hydrogels[41, 42]. Conversely, BC-PAA-1.0-0 shrank to 87.3% of its original volume and got tough at pH 2. BC-PAA-1.0-0 softened with swelling at high pH and stiffened with shrinking at low pH, showed a pH-responsive behavior similar to conventional PAA hydrogels, but exactly opposite to other prepared BC-PAA composite hydrogels.
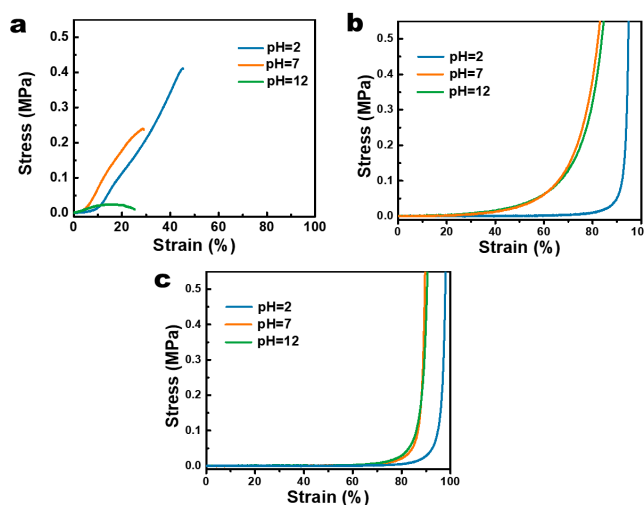
Fig. 3 Compression stress-strain curves of (a) BC-PAA-1.0-0, (b) BC-PAA-1.0-60, (c) BC-PAA-1.0-95 at pH 2, 7 and 12.

In comparison, BC-PAA-1.0-60 showed an ultra-soft state at pH 2 (**Fig. 3b**). The densification region appeared in the compression curve of BC-PAA-1.0-60 without prior stress increase, owing to the disappearance of interior osmotic pressure. On the other hand, with the increase of pH to 12, BC-PAA-1.0-60 did not show further stiffening than at pH 7, which can be ascribed to the pK_a of PAA, which was generally lower than 7. Thus, the ionization degree of the carboxylic groups did not increase significantly with the pH increasing to 12. With an extremely low amount of PAA, BC-PAA-1.0-95 gels showed similar pH-responsive behavior with BC-PAA-1.0-60 but in a

more inconspicuous way (**Fig. 3c**), which can be ascribed to its low carboxyl group amount. Moreover, because of the steady structure of the BC interior network, no obvious swelling or shrinkage was observed during the stiffness change both BC-PAA-1.0-60 and BC-PAA-1.0-95.

According to these results, it clearly showed that the pre-neutralization degree of the AA monomer would influence the content and morphology of grafted PAA in BC-*g*-PAA composite hydrogels. Meanwhile, the appropriate structure and amount of PAA in BC-PAA composite hydrogels are prerequisites for realizing effective mechanical adaptability in BC-*g*-PAA composite hydrogels.

Table 2 The compression properties and volume change ratio (VCR) of BC-PAA-2.0-60 at different pH.

pH	VCR[a] (%)	ε_b[b] (%)	σ_b[c] (MPa)	$\varepsilon_{0.1}$[d] (%)
2	-14.3	-	-	82.7±2.4
3	-13.3	-	-	79.4 ± 2.3
4	-12.6	83.3 ± 0.3	0.59 ± 0.07	66.1 ± 2.9
5	-9.2	77.4 ± 0.2	0.49 ± 0.02	57.2 ± 0.9
6	-6.4	66.5 ± 0.6	0.40 ± 0.03	49.1 ± 2.0
7	0	41.6 ± 0.1	0.23 ± 0.01	23.8 ± 1.2
10	0.4	46.2 ± 0.4	0.22 ± 0.01	25.7 ± 0.2
12	0.3	39.53 ± 1.5	0.16 ± 0.02	25.7 ± 0.9

a: volume change ratio, b: fractured strain, c: compression strength, d: strain at the stress of 0.1 MPa.

The pH-responsive behavior of BC-*g*-PAA hydrogels at various pH was further studied in BC-PAA-2.0-60. With the concentration of AA monomer increased from 1.0 to 2.0 mol L^{-1}, the content of PAA, which plays a pivotal role in mechanical properties and mechanical adaptivity of BC-*g*-PAA hydrogels, increased from 0.4 wt% in BC-PAA-1.0-60 to 1.2 wt% in BC-PAA-2.0-60.

As can be seen in **Fig. 4a**, BC-PAA-2.0-60 stiffened with the pH of surrounding solutions raising from 2 to 12. To be specific, when the pH increased from 2 to 7, BC-PAA-2.0-60 continuously stiffened. It was manifested in the compression curves that the strain hardening behavior occurred at lower strains with pH increasing. As a weak polyelectrolyte, the deprotonation degree of the carboxyl groups from PAA would increase with pH. The protons of carboxylic acid groups would diffuse to the surrounding solution, make the polymer backbone charged and cause a difference in osmotic pressure between the gel and surrounding solution, result in stiffening in the BC-PAA-2.0-60 hydrogels. In the case of a conventional pH-responsive hydrogel, the generation of osmotic pressure inside results in swelling as water permeates into the hydrogel network, which causes the hydrogel to become mechanically weaker or brittle[36, 41]. In stark contrast, the BC-*g*-PAA hydrogels showed stiffening

behavior without any obvious volume changes. For BC-*g*-PAA hydrogels, the interior highly developed nanocellulose network of BC acted as a steady scaffold to resist the swelling/shrinkage caused by osmotic pressure. Consequently, the swelling or shrinking ratio (volume change) of BC-PAA-2.0-60 at pH from 2 to 12 kept lower than 15% as recorded in **Table. 2**. Meanwhile, the generated osmotic pressure in BC-*g*-PAA hydrogel hardened the composite hydrogel consequently. As shown in **Table 2** and **Fig. 4a**, BC-PAA-2.0-60 sample stiffened with pH increase, became able to resist external compression rather than completely complying with external compression.

As the BC-PAA composite hydrogels were soft material, no definite moduli could be obtained from their compression curves. To evaluate the stiffness change of BC-PAA-2.0-60, the compression strains at a constant stress of 0.1 MPa (noted as $\varepsilon_{0.1}$) at different pH were recorded, which indicates the deformation extent of the samples under the same stress at different pH values. As shown in **Fig. 4b** and **Table 2**, $\varepsilon_{0.1}$ of BC-PAA-2.0-60 was 82.7% at pH 2, exhibited the high softness of BC-PAA-2.0-60 sample at pH 2, as a high deformation already occurred under low stress of 0.1 MPa. With the increase in pH from 2 to 7, $\varepsilon_{0.1}$ of BC-PAA-2.0-60 gradually decreased from 82.7% to 23.8%, showing a stiffening process of the BC-*g*-PAA hydrogels. Notably, $\varepsilon_{0.1}$ of BC-PAA-2.0-60 reached 23.8% at pH 7 but did not show further decreases with pH increased to 12. The acid dissociation constant (pK_a) of grafted PAA in BC-PAA-2.0-60 was confirmed as 6.2 through titration, which was generally agreed with other works[43, 44]. The ionization ratio of carboxylic acid groups could be estimated according to Henderson-Hasselbalch equation[45-47]. When pH increased to 7, the ionization ratio of carboxylic acid groups in PAA reached 86.3%, it was suggested that ionized carboxylate groups already occupied the majority. Thus, BC-PAA-2.0-60 showed an approximate linear elastic part after the compression strain reached 13.5% in the compression curve at pH 7. However, the ionization ratio of carboxylic acid groups in PAA was only 38.7% at pH 6. The hydrogel still maintained the softness, showed a $\varepsilon_{0.1}$ of 49.1% without obvious elastic deformation in the compression curve. In addition, owing to the probable disruption of H-bonding between nanocellulose in BC and PAA at pH 12, BC-PAA-2.0-60 was easier be crushed at pH 12 and showed a lower compression strength. These results showed that the prepared BC-PAA-2.0-60 hydrogels could respond to pH change and adjust their mechanical characteristics spontaneously without obvious volume change in a reversible way.

The reversibly pH-responsive BC-PAA-2.0-60 was used as a squat actuator to operate a 200-g weight (see **Fig. 4c**). BC-PAA-2.0-60 was immersed in about 100 ml pure water and retained its original thickness under a 200-g weight, showed a stiff state. With the addition of 1.0 ml of 1 mol L^{-1} HCl solution, the hydrogel gradually turned to its soft state in *c.a.* 20 min, while flattened and lifted down the weight horizontally and smoothly. Subsequently, 1.1 ml of 1 mol L^{-1} NaOH solution was added and turned the solution to alkaline. After the hydrogel reached its equilibrium state, BC-PAA-2.0-60 hydrogel almost completely recovered to the original thickness with lifting the weight up to

the original height, due to the regeneration of internal osmotic pressure. The reversible stiffness change-based unidirectional actuation implied that the BC-PAA-2.0-60 hydrogel could act as a squat actuator to lift weights reversibly in a controllable way. Meanwhile, the hydrogel would not show any obvious volumetric changes at different pH values without a weight as shown in **Fig. 4d**, owing to the steady structure of cellulose in BC.

3.3 Dual pH-responsiveness of BC-*g*-PAmph composite hydrogels

As above, the pH-responsive mechanically adaptivity of BC-*g*-PAA hydrogels can be generally described as monotonously hardening with pH increasing over pK_a. The work pattern of BC-*g*-PAA hydrogels may be restricted by this humdrum pH-responsive behavior to a certain extent. On the other hand, polyampholyte hydrogels composed of anionic and cationic groups showed larger variety in pH-responsive behavior, like the dual pH responsiveness, suggested higher working flexibility in a broader pH range[48]. Here, we copolymerized 2-(dimethylamino)ethyl methacrylate with acrylic acid to form a polyampholyte system, which was grafted onto BC and realized a dually pH-responsive behavior in the obtained BC-*g*-PAmph hydrogels (**Fig. 5a**).

To balance the charge between the cationic and anionic monomers, the molar ratio of DMAEMA to AA was 1:1 in the preparation of BC-*g*-PAmph hydrogels. **Fig. 5b** displays the FT-IR spectra of lyophilized BC-*g*-PAmph and BC-*g*-PAA hydrogels.

Compared with the IR spectra of BC-*g*-PAmph and BC-*g*-PAA hydrogels, the peak of C=O in carboxyl groups at 1705 cm^{-1} shifted to 1720 cm^{-1}, and a new peak at 1575 cm^{-1} appeared in BC-*g*-PAmph, indicating that the ionic bonds formed between the carboxyl groups from AA and ammonium groups from DMAEMA[48-50].

Table 3 The compression properties and volume change ratio (VCR) of BC-PAmph-0.75 at different pH.

pH	VCR[a] (%)	ε_b[b] (%)	σ_b[c] (MPa)	$\varepsilon_{0.1}$[d] (%)
2	0.2	78.7 ± 0.4	0.43 ± 0.01	56.4 ± 1.5
3	0.2	-	-	63.7 ± 0.2
5	0	-	-	68.7 ± 1.3
7	0	-	-	68.6 ± 1.3
8	0	-	-	68.2 ± 1.2
10	0	-	-	68.1 ± 1.0
11	0.2	76.7 ± 0.2	0.56 ± 0.03	52.3 ± 1.4
12	0.4	68.7 ± 1.0	0.37 ± 0.01	45.9 ± 2.3

a: volume change ratio, b: fractured strain, c: compression strength, d: strain at the stress of 0.1 MPa.
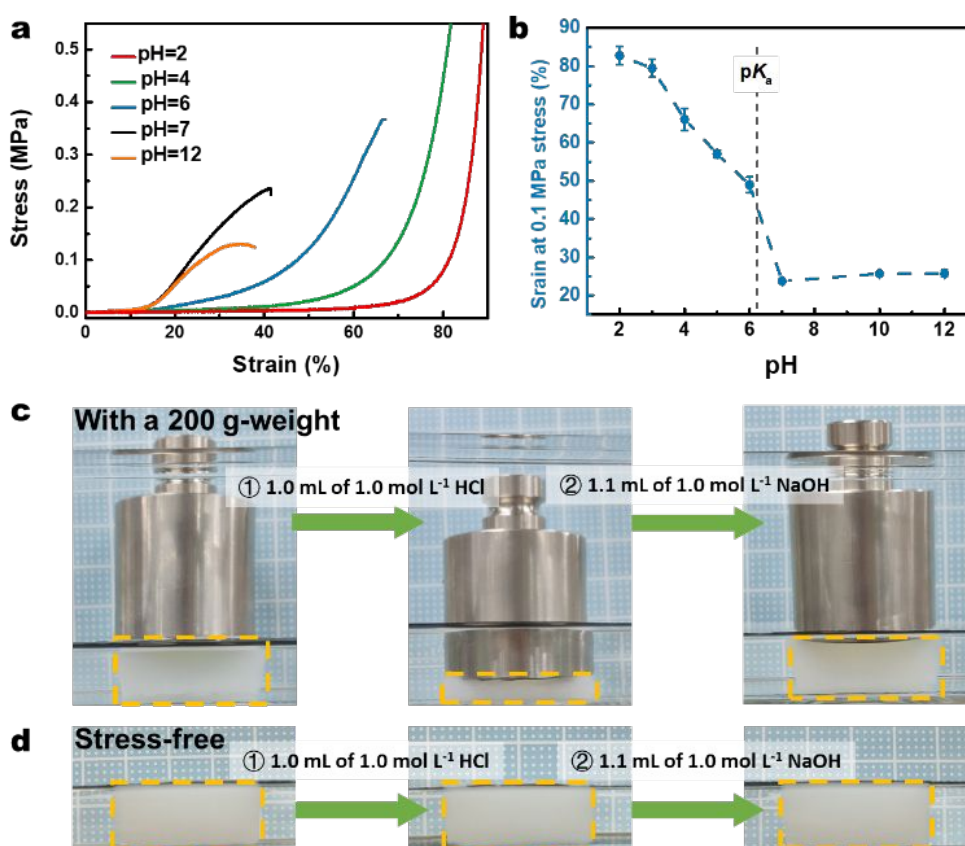
Fig. 4 (a) Compression curves of BC-PAA-2.0-60 at different pH. (b) Strain at 0.1 MPa stress in compression of BC-PAA-2.0-60 as a function of pH. (c) Utilizing the reversible pH-responsiveness of BC-PAA-2.0-60 to lift a 200 g-weight. (d) No obvious volumetric changes in BC-PAA-2.0-60 were showed without external pressure.

ARTICLE

Fig. 5c and **5d** show the pH-responsive compression properties of BC-PAmph-0.75, which prepared with a total monomer concentration of 0.75 mol L^{-1}, showed a typical dually pH-responsive behavior in compression. The compression stress-strain curves exhibited that BC-PAmph-0.75 was soft and flexible enough to sustain a high compression strain up to the testing limit in general conditions. However, it would lose its softness when pH increased over 11 or decreased to 2. As same as BC-g-PAA hydrogels, the strains of BC-PAmph-0.75 at a stress of 0.1 MPa ($\varepsilon_{0.1}$) in compression at different pH were also recorded as an indicator of stiffness in **Table 3**. The pH-induced $\varepsilon_{0.1}$ change was exhibited in **Fig. 5d**, which showed an inverted U shape curve. The $\varepsilon_{0.1}$ of BC-PAmph-0.75 is 68.6% at pH 7, showed no obvious changes at the pH interval from 5 to 10. When the pH decreased to 3, its $\varepsilon_{0.1}$ decreased to 63.7% and then decreased to 56.4% at pH 2. Moreover, the $\varepsilon_{0.1}$ of BC-PAmph-0.75 showed an abrupt decrease from pH 10 to pH 11 and further decreased to 45.9% at pH 12. The results suggested that the presence of the polyampholyte affords the BC-PAmph composite hydrogels capable of responding to pH in a dual way with stiffness change.

It is worth noting that the content of grafted polymer in BC-PAmph-0.75 was only 0.8 wt%, much lower than BC-PAA-2.0-

60, which had a PAA content of 1.2 wt% as reported above. However, BC-PAmph-0.75 did not show an ultra-soft state in the full pH range from 2 to 12, which was observed in BC-PAA-2.0-60 in acidic conditions. As the oppositely charged homo-polyelectrolytes could form strong and tough hydrogels[49, 51, 52], it is reasonable to hypothesize that interchain and intrachain ionic crosslinking would be formed between the carboxyl groups and ammonium groups in this randomly polymerized PAA-PDMAEMA polyampholyte (**Fig. 5e**). Therefore, the polymer network in BC-Pamph-0.75 was strengthened and no longer showed an ultra-soft state whatsoever. However, the ionic bonding between carboxyl groups and ammonium groups would be disrupted with pH increase and decrease, but the BC-PAmph hydrogel would be further strengthened. As illustrated in **Fig. 5e**, a certain portion of the carboxyl groups would be protonated in acidic circumstances, while the PDMAEMA remained in a charged form. The presence of positively charged ammonium groups increased the interior osmotic pressure in the hydrogel, which was converted to resisting forces in compression with the no swelling BC matrix. As a result, the stiffness of BC-PAmph increased, although the ionic binding between the ammonium group and carboxylic groups was partially disrupted. Similarly, the ammonium groups turned to
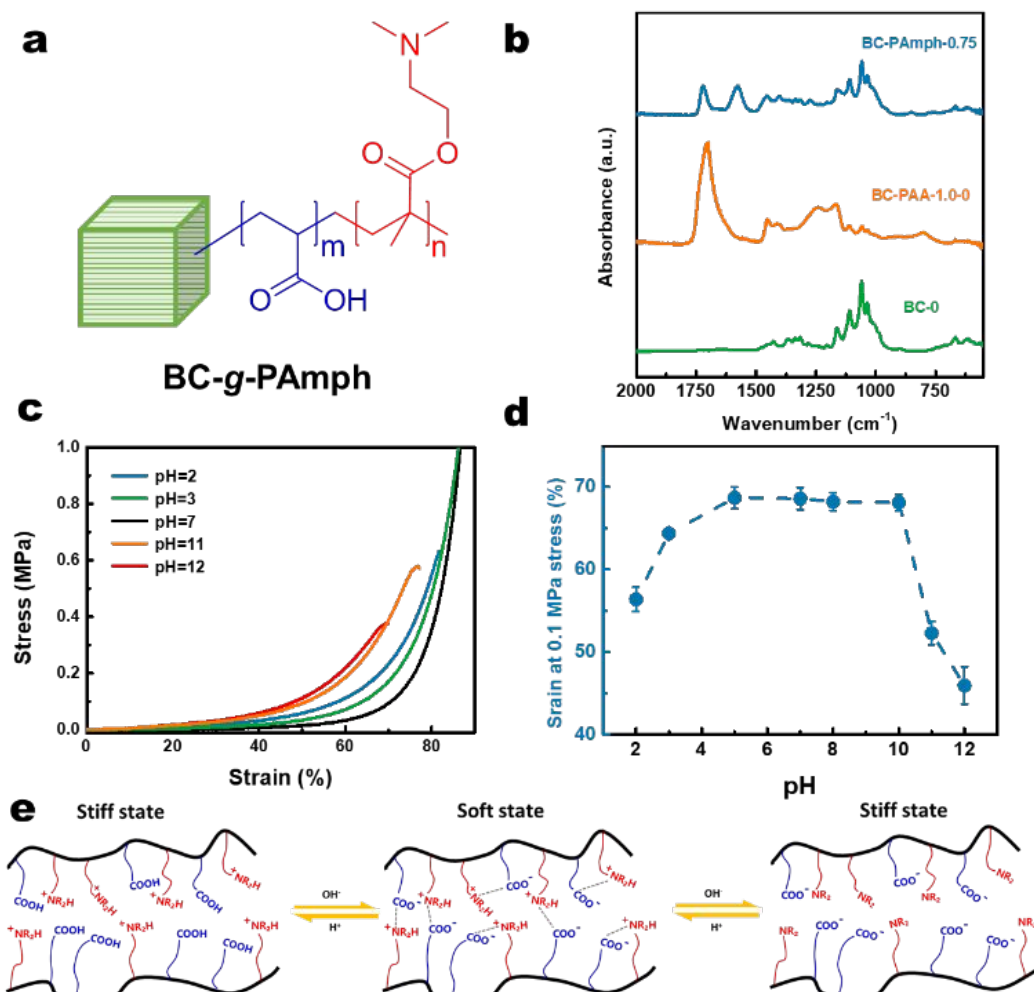
Fig. 5 (a) Chemical structure of BC-g-PAmph. (b) ATR-FTIR spectra of BC-PAA-1.0-0 and BC-PAmph-0.75. (c) Compression curves of BC-PAmph-0.75 at different pH. (d) Strain at 0.1 MPa stress in compression of BC-PAmph-0.75 as a function of pH. (e) The mechanism of dual-pH responsiveness of BC-g-polyampholyte hydrogels.

electrically neutral in alkaline circumstances while the carboxyl groups kept a negatively charged state, which also resulted in stiffening in BC-PAmph hydrogels. The results showed that the internal osmotic pressure dominated the stiffness of the BC composite hydrogels, which can be utilized to design various stiffness adjusting protocols.

3.4 UV-responsiveness of BC-PAA-2.0-60 composite hydrogel with 2-nitrobenzaldehyde

In contrast to other physical stimuli that can be applied or removed instantaneously, the actuation of pH-responsive materials highly associated with the diffusion process[53, 54]. Therefore, triggering BC-g-PAA hydrogels independently and quickly remains a challenge in potential practical applications.

From this regard, we utilized a photoacid generator with generated proton by photo-irradiation to decrease the local pH of the solution in BC-g-PAA hydrogel. As the schematic illustration in **Fig. 6a**, 2-nitrobenzaldehyde (NBA) can release protons upon UV irradiation[26, 53, 55], dramatically decrease pH inside the gel so that triggers the stiffness change of BC-PAA-2.0-60. Here, a BC-PAA-2.0-60 strip was firstly immersed in 0.01 mol L^{-1} NBA aqueous solution. After NBA dispersed into BC-PAA-2.0-60, the hydrogel strip could maintain a horizontally straight state due to its original high stiffness in non-acidic solution (**Fig. 6c**). A UV curing system (Eficet, 8332A, Japan) was used to irradiate the hydrogel strip, as illustrated in **Fig. 6b**. In this process, the protons were generated because of the pH jump reaction of NBA, and the hydrogel strip gradually softened and finally drooped down in 8 min, as shown in **Fig. 6d**. As the hydrogel was locally irradiated by UV, the limited shrinkage

occurred only at the irradiated position, although the obvious drooping of the hydrogel strip was observed. As same as the pH-responsive softening in acidic solution, the softened hydrogel strip here could also recover to the stiff state by washing with water or directly neutralizing with alkaline solutions.

Furthermore, integrating a pH-jump reaction into BC-g-PAA hydrogel makes it possible to realize spatial control of softness change, *i.e.*, spatial lift-down actuation is able. As shown in **Fig. 6e**, the NBA containing BC-PAA-2.0-60 hydrogel can withstand the compression of two weights (*c.a.* 50 g of each) at both ends without obvious deformations. UV was only irradiated and focused on the right end of the hydrogel (**Fig. 6f**) for 8 min. After the region-selective UV irradiation, the softening only happened at the right end of the hydrogel strip, as shown in **Fig. 6g**. The right end of BC-PAA-2.0- 60 was squished and lifted the 50 g-weight down without in-plane displacements, while the other weight kept its original height at the unexposed left end. This spatiotemporally unidirectional actuation was unable to be operated in common hydrogel actuators because of inevitable bulking.

The integration of NBA realized remote and rapid UV-response in BC-g-PAA hydrogel, meanwhile could weaken the dependency of its mechanical adaptivity on an external solution in further applications. Moreover, the remote UV stimulus could be transformed local signals in hydrogel and realize spatiotemporally controllable mechanical property change and actuation. The combination of pH-jump system and pH-responsive mechanically adaptive BC composite hydrogel will provide opportunities for designing predictive and programmable hydrogel structural devices and actuators.

4. Conclusions

In summary, a new class of stimuli-responsive stiffness adjustable BC composite hydrogels was prepared by grafting pH-responsive polymers on the surface of BC nanofibers. After grafting PAA to BC, the stiffness of BC-g-PAA hydrogel could be reversibly adjusted by pH, owing to the pH-responsibility of PAA. Meanwhile, the potential volumetric changes in the mechanical adjusting process could be well suppressed by the steady structure of BC. Utilizing the unique property of BC-g-PAA hydrogel, a prototype of squat actuator was designed to lift a weight up and down in a controllable manner. To extend the pH-responsive protocol, PDMAEMA was also introduced and formed a polyampholyte with PAA in BC composite hydrogel. The obtained BC-g-Polyampholyte hydrogel showed a dual pH-responsibility, not only stiffened at basic pH but also at acidic pH.

Furthermore, a photoacid generator, 2-nitrobenzaldehyde, was used to trigger UV-controlled softening in BC-g-PAA, realized a surrounding solution-independent remote control in these pH-responsive BC composite hydrogels. For specific interests in predictive and programmable soft structure, the partial softening and actuation of BC-g-PAA as a structural device can be activated by selective UV irradiation.

Fig. 6 (a) Photochemistry mechanism of 2-nitrobenzaldehyde. (b) Illustration of UV irradiation on BC-PAA-2.0-60 strip. (c, d) Photographs of UV-initiated softening of BC-PAA-2.0: the horizontally straight BC-PAA-2.0-60 hydrogel strip hung down after UV irradiation. (e, f, g) Spatial control of BC-PAA-2.0 softening by UV: two weights (*c.a.* 50 g) were put on both ends of BC-PAA-2.0-60 strip; UV irradiation was only applied to the right end of hydrogel strip; the height difference of the two weights showed the difference in stiffness between the two ends of BC-PAA-2.0-60 strip.

The success in preparing these low swelling stimuli-responsive BC composite hydrogels confirmed the general availability of the design, which uses BC as a steady matrix scaffold and free-chain stimuli-responsive polymer as an osmotic pressure generator. It is also envisioned that this study might open new opportunities to develop other smart hydrogels for soft actuators.

Conflicts of interest

There are no conflicts to declare.

Acknowledgements

Notes and references

1. E. L. Wang, Y. B. Dong, M. Z. Islam, L. M. Yu, F. Y. Liu, S. J. Chen, X. M. Qi, Y. F. Zhu, Y. Q. Fu, Z. H. Xu and N. Hu, *Composites Science and Technology*, 2019, **169**, 209-216.
2. M. A. Stuart, W. T. Huck, J. Genzer, M. Muller, C. Ober, M. Stamm, G. B. Sukhorukov, I. Szleifer, V. V. Tsukruk, M. Urban, F. Winnik, S. Zauscher, I. Luzinov and S. Minko, *Nat Mater*, 2010, **9**, 101-113.
3. C. Qian, Y. B. Dong, Y. F. Zhu and Y. Q. Fu, *Smart Materials and Structures*, 2016, **25**, 085023.
4. Z. Shi, X. Shi, M. W. Ullah, S. Li, V. V. Revin and G. Yang, *Advanced Composites and Hybrid Materials*, 2017, **1**, 79-93.
5. H. Qin, T. Zhang, N. Li, H. P. Cong and S. H. Yu, *Nat Commun*, 2019, **10**, 2202.
6. M. Kato, T. A. Asoh and H. Uyama, *Chem Commun (Camb)*, 2019, **55**, 4170-4173.
7. H. Wang and S. C. Heilshorn, *Adv Mater*, 2015, **27**, 3717-3736.
8. G. Li, Y. P. Wang, S. W. Wang and J. Q. Jiang, *Macromolecular Materials and Engineering*, 2018, **303**.
9. T. A. Asoh and M. Akashi, *Chem Commun (Camb)*, 2009, DOI: 10.1039/b905791a, 3548-3550.
10. L. Montero de Espinosa, W. Meesorn, D. Moatsou and C. Weder, *Chem Rev*, 2017, **117**, 12851-12892.
11. Z. G. Zhao, Y. C. Xu, R. C. Fang and M. J. Liu, *Chinese Journal of Polymer Science*, 2018, **36**, 683-696.
12. J. B. Lee, S. Peng, D. Yang, Y. H. Roh, H. Funabashi, N. Park, E. J. Rice, L. Chen, R. Long, M. Wu and D. Luo, *Nat Nanotechnol*, 2012, **7**, 816-820.
13. H. Xing, Z. Li, Z. L. Wu and F. Huang, *Macromol Rapid Commun*, 2018, **39**.
14. F. Gao, Y. Zhang, Y. Li, B. Xu, Z. Cao and W. Liu, *ACS Appl Mater Interfaces*, 2016, **8**, 8956-8966.
15. N. Kong, Q. Peng and H. B. Li, *Advanced Functional Materials*, 2014, **24**, 7310-7317.
16. H. Meng, J. Zheng, X. Wen, Z. Cai, J. Zhang and T. Chen, *Macromol Rapid Commun*, 2015, **36**, 533-537.
17. H. Kamata, K. Kushiro, M. Takai, U. I. Chung and T. Sakai, *Angew Chem Int Ed Engl*, 2016, **55**, 9282-9286.
18. H. Kamata, Y. Akagi, Y. Kayasuga-Kariya, U. I. Chung and T. Sakai, *Science*, 2014, **343**, 873-875.
19. J. K. Nguyen, D. J. Park, J. L. Skousen, A. E. Hess-Dunning, D. J. Tyler, S. J. Rowan, C. Weder and J. R. Capadona, *J Neural Eng*, 2014, **11**, 056014.
20. S. Wei, W. Lu, X. Le, C. Ma, H. Lin, B. Wu, J. Zhang, P. Theato and T. Chen, *Angew Chem Int Ed Engl*, 2019, **58**, 16243-16251.
21. Z. Hu, X. Zhang and Y. Li, *Science*, 1995, **269**, 525-527.
22. J. Shang, X. Le, J. Zhang, T. Chen and P. Theato, *Polymer Chemistry*, 2019, **10**, 1036-1055.
23. T. A. Asoh, M. Matsusaki, T. Kaneko and M. Akashi, *Advanced Materials*, 2008, **20**, 2080-+.
24. J. Zheng, P. Xiao, X. X. Le, W. Lu, P. Theato, C. X. Ma, B. Y. Du, J. W. Zhang, Y. J. Huang and T. Chen, *J. Mater. Chem. C*, 2018, **6**, 1320-1327.
25. B. Y. Wu, X. X. Le, Y. K. Jian, W. Lu, Z. Y. Yang, Z. K. Zheng, P. Theato, J. W. Zhang, A. Zhang and T. Chen, *Macromol Rapid Commun*, 2019, **40**, e1800648.
26. P. Techawanitchai, M. Ebara, N. Idota, T. A. Asoh, A. Kikuchi and T. Aoyagi, *Soft Matter*, 2012, **8**, 2844-2851.
27. H. Ko and A. Javey, *Acc Chem Res*, 2017, **50**, 691-702.
28. T. A. Asoh and A. Kikuchi, *Chem Commun (Camb)*, 2010, **46**, 7793-7795.
29. C. Yao, Z. Liu, C. Yang, W. Wang, X. J. Ju, R. Xie and L. Y. Chu, *ACS Appl Mater Interfaces*, 2016, **8**, 21721-21730.
30. C. Ma, T. Li, Q. Zhao, X. Yang, J. Wu, Y. Luo and T. Xie, *Adv Mater*, 2014, **26**, 5665-5669.
31. Z. J. Wang, C. N. Zhu, W. Hong, Z. L. Wu and Q. Zheng, *Sci Adv*, 2017, **3**, e1700348.
32. X. Peng, Y. Li, Q. Zhang, C. Shang, Q. W. Bai and H. L. Wang, *Advanced Functional Materials*, 2016, **26**, 4491-4500.
33. C. Qian, T. A. Asoh and H. Uyama, *Chem Commun (Camb)*, 2018, **54**, 11320-11323.
34. M. Iguchi, S. Yamanaka and A. Budhiono, *Journal of Materials Science*, 2000, **35**, 261-270.
35. M. M. Abeer, M. C. Mohd Amin and C. Martin, *J Pharm Pharmacol*, 2014, **66**, 1047-1061.
36. M. C. Koetting, J. T. Peters, S. D. Steichen and N. A. Peppas, *Mater Sci Eng R Rep*, 2015, **93**, 1-49.
37. S. S. Cuti, P. B. Smith, D. E. Henton, T. L. Staples and C. Powell, *Journal of Polymer Science Part B: Polymer Physics*, 1997, **35**, 2029-2047.
38. P. Drawe, M. Buback and I. Lacik, *Macromolecular Chemistry and Physics*, 2015, **216**, 1333-1340.
39. D. Benda, J. Snuparek and V. Cermak, *European Polymer Journal*, 2001, **37**, 1247-1253.
40. L. Cai and S. Wang, *Biomacromolecules*, 2010, **11**, 304-307.
41. L. Arens, F. Weissenfeld, C. O. Klein, K. Schlag and M. Wilhelm, *Adv Sci (Weinh)*, 2017, **4**, 1700112.
42. X. W. Peng, J. L. Ren, L. X. Zhong, F. Peng and R. C. Sun, *J Agric Food Chem*, 2011, **59**, 8208-8215.
43. B. N. Dickhaus and R. Priefer, *Colloids and Surfaces A: Physicochemical and Engineering Aspects*, 2016, **488**, 15-19.
44. Y. Hoshino, T. Jibiki, M. Nakamoto and Y. Miura, *ACS Appl Mater Interfaces*, 2018, **10**, 31096-31105.

45. E. Bombarda and G. M. Ullmann, *J Phys Chem B*, 2010, **114**, 1994-2003.
46. E. P. Lai, Y. X. Wang, Y. Wei, G. Li and G. H. Ma, *Macromolecular Chemistry and Physics*, 2017, **218**.
47. W. Tao, J. Q. Wang, W. J. Parak, O. C. Farokhzad and J. J. Shi, *Acs Nano*, 2019, **13**, 4876-4882.
48. G. Li, G. P. Zhang, R. Sun and C. P. Wong, *Polymer*, 2016, **107**, 332-340.
49. J. You, S. Y. Xie, J. F. Cao, H. Ge, M. Xu, L. N. Zhang and J. P. Zhou, *Macromolecules*, 2016, **49**, 1049-1059.
50. R. I. Moustafine, T. V. Kabanova, V. A. Kemenova and G. Van den Mooter, *J Control Release*, 2005, **103**, 191-198.
51. F. Luo, T. L. Sun, T. Nakajima, D. R. King, T. Kurokawa, Y. Zhao, A. Bin Ihsan, X. F. Li, H. L. Guo and J. P. Gong, *Macromolecules*, 2016, **49**, 2750-2760.
52. B. Xu, X. Zhang, S. C. Gan, J. H. Zhao and J. H. Rong, *Journal of Materials Science*, 2019, **54**, 14218-14232.
53. M. Ebara and T. Aoyagi, *Journal of Photopolymer Science and Technology*, 2014, **27**, 467-469.
54. P. Techawanitchai, N. Idota, K. Uto, M. Ebara and T. Aoyagi, *Sci Technol Adv Mater*, 2012, **13**, 064202.
55. Y. Kotsuchibashi, M. Ebara, T. Sato, Y. Wang, R. Rajender, D. G. Hall, R. Narain and T. Aoyagi, *J Phys Chem B*, 2015, **119**, 2323-2329.
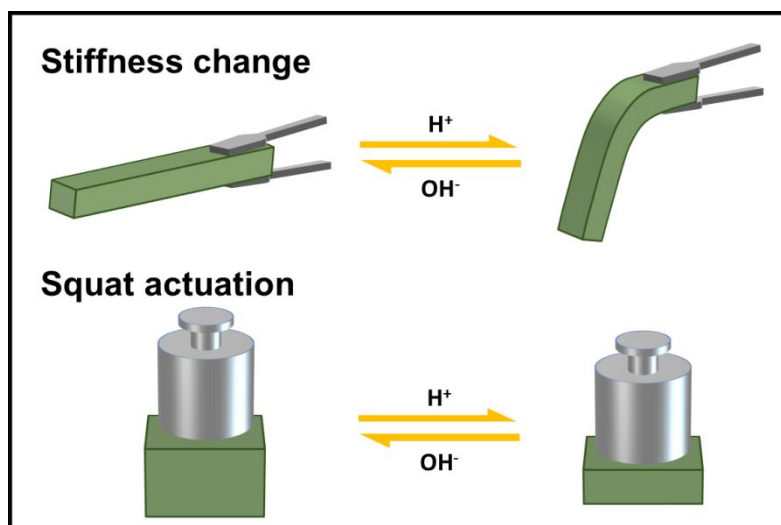
Stimuli-responsive stiffness change and squat actuation were realized in bacterial cellulose hydrogel by utilizing internal osmotic pressure change.